International Journal of Scientific Research in Engineering and Management (IJSREM)
Volume: 09 Issue: 12 | Dec - 2025 SJIF Rating: 8.586 ISSN: 2582-3930

Comparative CFD Analysis of Twisted-Tape Swirling Jet and Conventional Impinging Jet for Heat Transfer Enhancement

Mr. Jaspreet Singh[1] , Dr. Rakesh Kumar[2] , Ms. Saloni Spall[3] , Mr. Jagjit Singh[4]

Assistant Professor, Mechanical, LGC, Chaukiman, Ludhiana, India [1]
Principal, Mechanical, LGC, Chaukiman, Ludhiana, India [2]
Assistant Professor, Mechanical, LGC, Chaukiman, Ludhiana, India [3]
Assistant Professor, Mechanical, LGC, Chaukiman, Ludhiana, India [4]

Abstract: This paper reports the computational fluid dynamics (CFD) modelling of heat transfer analysis from a heated target surface, using single swirling jet air impingement at different Reynolds numbers. Swirl is produced by using a nozzle body with half-length downstream twisted tape insert (HLDI). The nozzle to plate (target surface) distance and twist ratio (y) of twisted tape is taken to be constant as 21mm (H/D = 1) and y = 2.93 respectively. Different Reynolds numbers as 12000, 17000, 22000 and 27000 are used to investigate the heat transfer characteristics on heated surface.

Key words: CFD, Swirling jet, Reynolds number, Heat transfer.

1.Introduction

Jet impingement is one of the most active techniques for heat transfer enhancement. Because of high heat transfer rate and other advantages, the technique has been widely used in many engineering and other areas for example cooling of turbine blades, chemical vapour deposition, drying of food products, cooling of hot steel plate, tempering of glass, papers, textiles and films, cooling of electronic equipment, and cooling of outer wall of the combustion chamber. Large quantity of literature is available on different configurations as single, row, and array of jets with co-relations developed for heat and mass transfer characteristics related to this field. The major disadvantage of conventional jet impingement is that the local heat flux can be highly non-uniform (Viskanta, 1993) [1]. To overcome this problem of radial non-uniformity several attempts have been made with different configurations. The introduction of swirl in the jet solved this problem up to much extent. Ward and Mahmood (1982)[2] showed that a swirling jet provided more uniform radial distribution of heat transfer as compared to non-swirling jet. A number of experimental, empirical and numerical studies have been conducted. Excellent review papers (Viskanta, (1987)[3] and (Zuckerman and Lior, (2006)[4] were published highlighting different issues. Carefully controlled experiments are required to improve the understanding of heat transfer characteristics from the impingement plate. Huan and Genk (1996)[5] conducted experiments to investigate and compare the performance of swirling and multi-channel impinging jets with that of a conventional impinging jet (CIJ), having the same diameter at the same conditions. Salce and Simon (1991)[6] also tried to visualize the swirl air flow inside a cylindrical cavity using the smoke wires technique. The images of the flow field, however, were not clear and did not show the whole flow field as compared to the Shlienand Hussain (1983)[7] Different techniques are used by different 0heat transfer coefficient. One of the experimental techniques is thermo chromic liquid crystal (TLC). This method is used by Nuntadusit, and Wae-hayee (2012)[8]. Flow and heat transfer characteristics of swirling impinging jet (SIJ) were studied experimentally at constant nozzle-to-plate distance of L=4D. Hunag et al. (1998)[9] used a swirl generator made of cylindrical plug with four narrow channels to provide swirl to single and multiple air impinging jets. It has been observed that swirling impinging jet (SIJ) demonstrated large increase in Nusselt number and significant improvement in radial uniformity of heat transfer as compared to multi-channel impinging jets (MCIJ) and conventional impinging jet (CIJ) which is contrary to results observed by Ward and Mahmood (1982)[10] and Lee et al. (2002)[11]. This was attributed to the fact that turbulence generated due to sudden

2. Numerical Setup

This study compares a conventional impinging jet (CIJ) with a twisted-tape swirling impinging jet (SIJ) using 3D CFD simulations. FLUENT 6.3.26 was used to model the pipe–nozzle–plate assembly. Air flows through a 21 mm diameter tube and impinges on a flat plate subjected to a uniform heat flux of 3000 W/m². In the swirling configuration, a half-length downstream insert (HLDI) twisted tape of 300 mm is placed inside the tube to generate swirl, whereas in the CIJ case the tape is removed to provide a purely axial jet. Both configurations were analyzed at Reynolds numbers 12,000, 17,000, 22,000, and 27,000 using identical numerical settings to ensure consistent comparison. This approach enables a direct evaluation of swirl-induced enhancement.

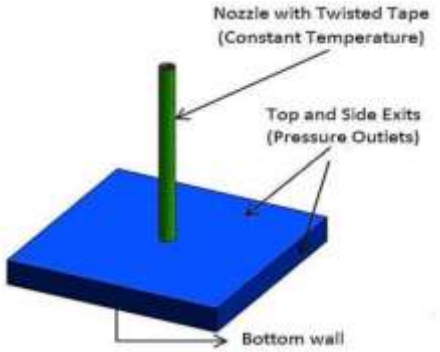

Fig.1Entire pipe-plate assembly

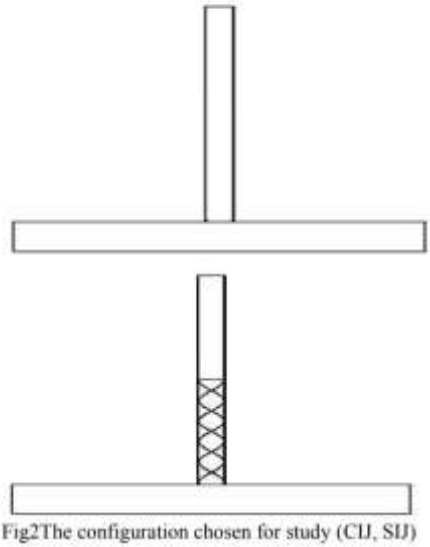
Fig2The configuration chosen for study (CIJ, SIJ)

3. Numerical Simulation

Fig. 3 shows the computational domain used for the numerical simulations performed in FLUENT 6.3.26. Table 1 summarizes the boundary conditions applied at different regions of the domain.

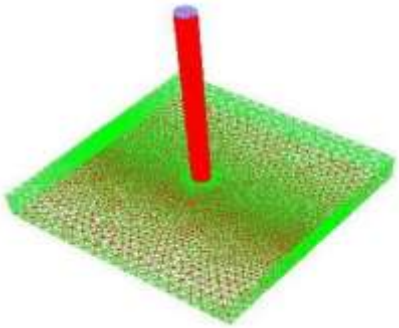
Fig. 3 computational domain

The mesh contains approximately 1.25 × 10^6 cells, which was found adequate to resolve the flow and thermal fields for both the conventional impinging jet (CIJ) and twisted tape swirling jet (SIJ) configurations. A second-order discretization scheme is used for all terms influencing heat transfer. Pressure is discretized using the second-order scheme, while second-order upwind is applied for momentum, turbulence kinetic energy, specific dissipation rate, and energy equations. The SIMPLE algorithm is adopted for pressure–velocity coupling. Simulations are performed in the steady-state mode with a convergence criterion of 10^{-5} for residuals and a maximum of 1000 iterations, adjustable if needed. The three-dimensional continuity, momentum and energy equations are solved along with the SST k–ω turbulence model, selected for its proven accuracy, stability and suitability for swirling and impinging jet flows. Identical numerical settings are applied for both CIJ and SIJ cases to ensure fair comparison of flow and heat-transfer characteristics.

Table 1.Boundary condition

Physical Location/ Geometrical Identity	Boundary Type	Colour
Top Surface/Opening/Outlet	Pressure Outlet	Green
Bottom Surface/ Impingement Plate	Wall	Red
Side/ Opening/ Outlet	Pressure Outlet	Green
Centre/Twisted Tape	Wall	Red
Inlet/Nozzle Inlet	Velocity Inlet	Blue
Nozzle Wall	Wall	Red

4. Governing Equations For Heat Transfer

Heat transfer from solid boundary to moving fluids can be described using Newton's law of cooling:

$$q = h(T_\infty - T_S) \quad (1)$$

where, 'q' is the heat flux from the solid to the fluid, 'h' is the heat transfer coefficient, 'T_∞' is the temperature of the bulk of the fluid and 'T_S' is the temperature of the solid surface. The temperature difference between the solid surface and the bulk of the fluid is the driving force for convection. The heat transfer coefficient 'h' is often non dimensionalized using the thermal conductivity 'k_t' and length scale 'D' which characterizes the geometry. This results in a non-dimensional number called Nusselt's number (Nu):

$$Nu = \frac{hD}{k_t} \quad (2)$$

The Nusselt's number (Nu) is often a complex function of the geometry, the flow velocity and the physical properties of the fluid. Usually, correlations are derived between the Nusselt's number (Nu), Reynolds number (Re), Prandtl number (Pr) and a non-dimensional function of geometry.

$$Pr = \frac{\mu c_p}{k_t} \quad (3)$$

So,

$$Nu = \frac{q}{(T_\infty - T_S)} \cdot \frac{Pr}{\mu c_p} \cdot D \quad (4)$$

5. Grid Dependency Test

A grid dependency test was performed to evaluate the influence of mesh refinement on the numerical results. The

baseline conventional impinging jet (CIJ) at Re = 12,000 and H/D = 2 was used for this assessment. Several meshes with increasing cell counts were generated, and the maximum Nusselt number on the impinged surface was monitored as the key comparison parameter. Coarser meshes showed noticeable variation, whereas further refinement produced only small changes in the predicted values. Based on this trend, a mesh containing approximately 1.2–1.3 million cells was selected for all simulations, ensuring adequate resolution and providing consistent accuracy for both the CIJ and twisted-tape swirling jet (SIJ) configurations.

Table 2.Grid dependency results

Sr. No.	Number of Cells	Nusselt Number
1	7,80,320	79.2
2	9,85,412	92.5
3	10,84,760	105.8
4	12,21,430	121.3
5	13,40,980	131.7
6	14,58,120	133.9
7	16,00,450	134.6
8	17,20,300	134.8

6. Swirling Impinging Jet (SIJ) And Conventional Impinging Jet (CIJ): Simulation And Results

1. Nusselt Number at Stagnation (X/D = 0)

The The stagnation point (X/D = 0) is the location where the jet directly impinges on the surface, resulting in maximum normal momentum and strong local convection. The Nusselt number at this point increases with Reynolds number for both CIJ and SIJ. Owing to enhanced swirl, improved mixing, and higher pre-impingement turbulence, the SIJ consistently exhibits greater stagnation Nusselt values than the CIJ. As seen from the data, the SIJ stagnation Nusselt numbers rise from 98.2 at Re = 12,000, to 130.5 at 17,000, 139 at 22,000, and 153 at 27,000, whereas the corresponding CIJ values increase from 48.8, 58.9, 66.2, to 73.3. These increasing trends, also reflected in the bar graph, highlight the stronger heat-transfer capability of the swirling jet.

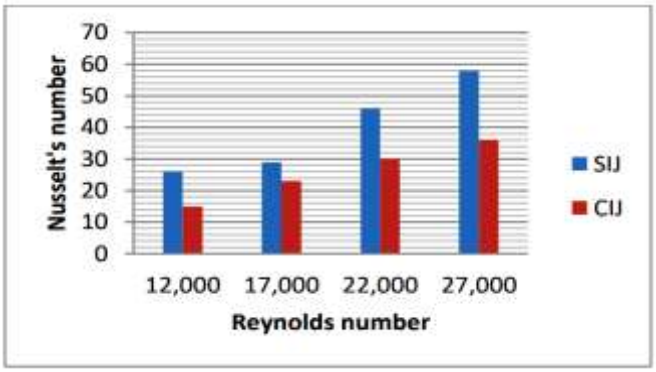

2. Nusselt Number at Peak Location

As the jet spreads radially, a secondary peak in the Nusselt number emerges at locations where wall shear and turbulence intensify. This peak often exceeds the stagnation value, particularly for SIJ, because the imposed swirl enhances radial transport and near-wall mixing. The variation of peak Nusselt numbers with Reynolds number clearly reflects this behavior: for SIJ, the values increase from 169 at Re = 12,000, to 211 at 17,000, 234 at 22,000, and 243 at 27,000. In comparison, CIJ exhibits lower peaks of 84.7, 95.7, 107.2, and 120.4 at the same respective Reynolds numbers, highlighting the superior heat transfer augmentation achieved by swirling jets.

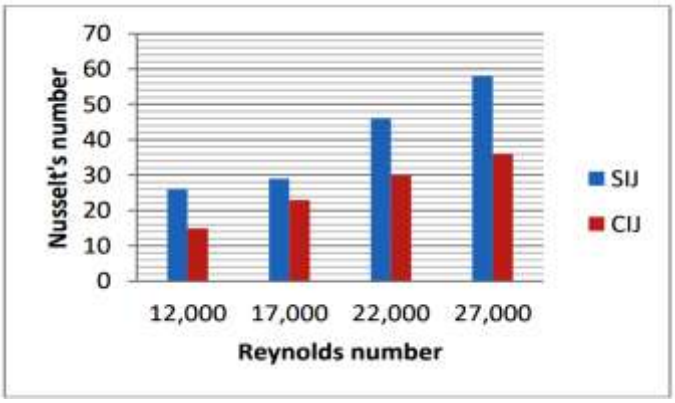

3. Average Nusselt Number

The average Nusselt number represents the overall heat transfer performance across the impingement surface. SIJ consistently yields higher average values than CIJ at all Reynolds numbers because the swirling motion promotes stronger mixing and distributes the jet momentum over a wider effective area. From the results, the SIJ average Nusselt number increases from 22 at Re = 12,000, to 31 at 17,000, 37 at 22,000, and 46 at 27,000. In comparison, the CIJ values rise more modestly from 12, 18, 22, to 28 across the same Reynolds numbers. These trends clearly demonstrate the superior overall heat-transfer capability of the swirling jet.

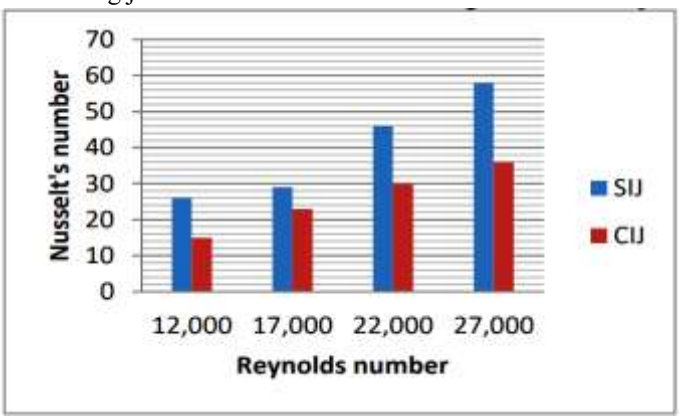

4. Heat-Transfer Coefficient at Stagnation

The stagnation heat-transfer coefficient represents the convective strength directly beneath the jet core, where the flow impinges with maximum intensity. As the Reynolds number increases, the stagnation h values rise for both SIJ and CIJ; however, SIJ consistently achieves higher values because swirl generates stronger turbulence and mixing before impact. From the results, the SIJ stagnation heat-transfer coefficient increases from 121.6 at Re = 12,000, to

161.5 at 17,000, 172 at 22,000, and 189.5 at 27,000, whereas the corresponding CIJ values increase from 60.4, 72.9, 81.9, to 90.8. These trends, also reflected in the bar graph, clearly demonstrate the enhanced convective performance of the swirling jet.

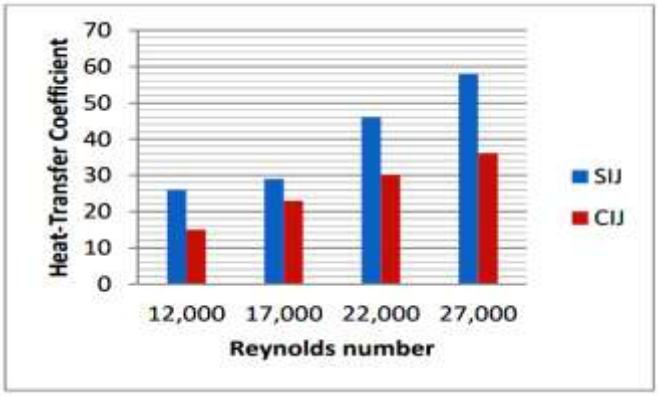

5. Heat-Transfer Coefficient at Peak Location

At radial positions away from the stagnation point, the flow transitions into a wall jet, where increased shear generates a distinct peak in the heat-transfer coefficient. This effect becomes even stronger in SIJ because swirl enhances radial momentum transport and near-wall turbulence, resulting in higher peak h values than those of CIJ. Based on the results, the SIJ peak heat-transfer coefficient increases from 209.1 at Re = 12,000, to 261.3 at 17,000, 289.5 at 22,000, and 300.7 at 27,000, while the corresponding CIJ values rise from 104.9, 118.4, 132.7, to 149. These values also reflected in the bar graph highlight the significantly improved wall-jet heat-transfer performance achieved by the swirling jet.

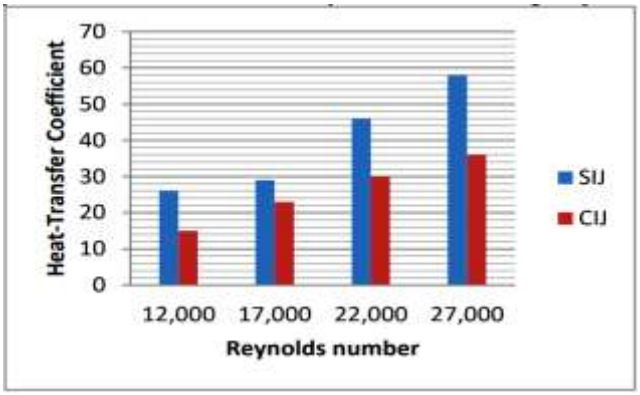

6. Average Heat-Transfer Coefficient

The average heat-transfer coefficient represents the overall thermal performance of the jet across the entire impingement surface. SIJ consistently maintains higher average h values than CIJ at all Reynolds numbers, reaffirming the swirl-induced enhancement in mixing and momentum distribution. From the results, the SIJ average heat-transfer coefficient increases from 26 at Re = 12,000, to 29 at 17,000, 46 at 22,000, and 58 at 27,000, whereas the corresponding CIJ values rise from 15, 23, 30, to 36. These trends, which are also reflected in the bar graph, clearly demonstrate the superior overall heat transfer capability of the swirling jet.

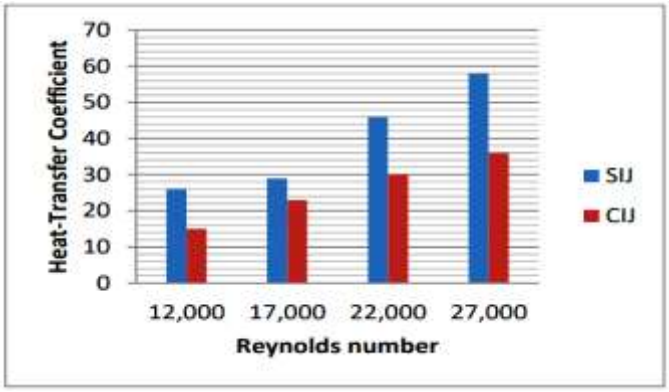

7. Conclusion

The present study demonstrates that introducing swirl through a twisted-tape insert significantly enhances the heat-transfer performance of an impinging jet compared to a conventional jet configuration. The swirl strengthens turbulence, improves core-to-wall mixing, and spreads the jet momentum more effectively over the target plate. As a result, the SIJ consistently exhibits higher Nusselt numbers and heat-transfer coefficients at the stagnation point, peak radial location, and over the entire surface.

The results show a clear increase in all heat-transfer parameters with increasing Reynolds number for both CIJ and SIJ. However, the rate of enhancement achieved by SIJ becomes more pronounced at higher Reynolds numbers due to stronger swirl penetration and higher turbulence energy in the wall-jet region. Average Nusselt number and average heat-transfer coefficient values confirm that swirl produces a broader and more effective impingement zone compared to the conventional jet.

Overall, the SIJ configuration provides a reliable passive method for thermal augmentation without increasing jet diameter or requiring additional energy input. This makes the swirling jet a promising option for applications where compact, high-performance cooling is required.

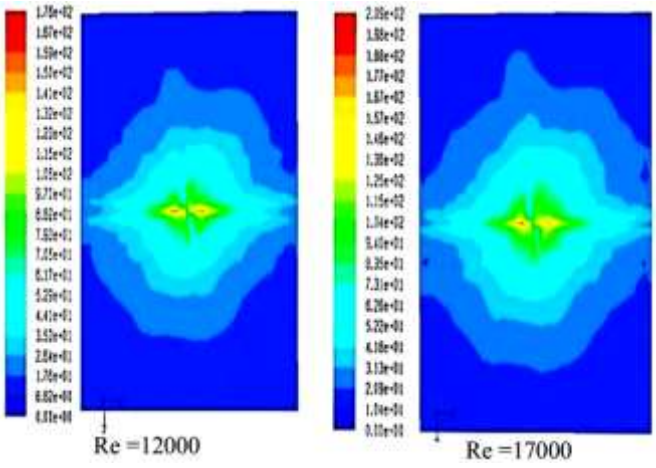

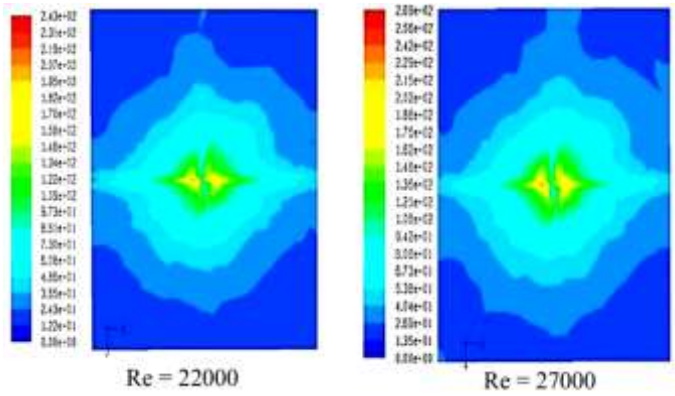

Fig. 4: Map of Nusselt number contours at different Reynolds number

Nomenclature D :

Diameter of the nozzle (m)

h : Local heat-transfer coefficient (W/m²·K)

k : Thermal conductivity of air (W/m·K)

Nu : Local Nusselt number

q* : Convective heat flux

r : Radial distance measured from the stagnation point

X/D : Non-dimensional radial position

Re : Reynolds number defined using nozzle diameter,

u : Average exit velocity of the jet (m/s)

ρ : Density of air (kg/m³)

μ : Kinetic viscosity of air (kg/m·s)

Acknowledgment

The author extends sincere appreciation to **Mr. Rakesh Kumar, Mr. Parampreet Singh, Mr. Jagjit Singh** and **Mr. Kawalpreet Singh** for their valuable discussions and support throughout this work.

References

[1] Jambunathan, K., Lai, E., Moss, M.A., Button, B.L. (1992). "A review of heat transfer data for single circular jet impingement," International Journal of Heat and Fluid Flow, 13, 106–115.

[2] Lytle, D., Webb, W. (1994). "Air-jet impingement heat transfer at low nozzle-plate spacings," International Journal of Heat and Mass Transfer, 37, 1687–1697.

[3] Viskanta, R. (1993). "Heat transfer to impinging isothermal gas and flame jets," Experiments in Thermal and Fluid Sciences, 6, 111–134.

[4] Ward, J., Mahmood, M. (1982). "Heat transfer from a turbulent, swirling impinging jet," 7th International Heat Transfer Conference, HTD-3, 401–407.

[5] Huang, L., El-Genk, M.S. (1998). "Heat transfer and flow visualization experiments of swirling, multi-channel, and conventional impinging jets," International Journal of Heat and Mass Transfer, 41, 583–600.

[6] Nuntadusit, C., Wae-hayee, M., Bunyajitradulya, A., Eiamsa-ard, S. (2012). "Visualization of flow and heat transfer characteristics for swirling impinging jet," International Communications in Heat and Mass Transfer, 39, 640–648.

[7] Xu, L., Yang, T., Sun, Y., Xi, L., Gao, J., Li, Y. (2021). "Flow and heat transfer characteristics of a swirling impinging jet issuing from a threaded nozzle of 45°," Energies, 14, 8412. [8] "Numerical and Experimental Studies on Heat Transfer Enhancement in a Circular Tube Inserted with Twisted Tape Inserts," American Journal of Energy Engineering, 9(2), 2021. [9] "Heat transfer of swirling impinging jets ejected from nozzles with twisted tapes CFD technique," Case Studies in Thermal Engineering.

[10] "A Review of Heat Transfer Enhancement Using Twisted Tape With and Without Perforation," International Journal of Innovations in Engineering Research and Technology (IJIERT), 2017.

[11] "Heat transfer in pipes with twisted tapes: CFD simulations and validation," Computers & Chemical Engineering, 2022.